

A single field inflationary potential consistent with recent observations

Md. Wali Hossain^{id}^a

^aDepartment of Physics, Jamia Millia Islamia,
New Delhi 110025, India

E-mail: mhossain@jmi.ac.in

Abstract. Current observations indicate that an inverse exponential form of the inflaton potential provides an excellent description of single-field inflation. This potential fits the SPA+BK+DESI data sets well with in the 1σ bound in the n_s-r plane, thereby offering a simple and observationally viable single field inflationary scenario. To describe post-inflationary evolution and reheating, we extend the inverse-exponential potential by adding a steep exponential term that remains negligible during inflation but becomes important afterwards. The resulting full potential develops a minimum after the end of inflation, leading to oscillations of the scalar field and consequently reheating of the Universe. We find that the maximum reheating temperature attainable in this scenario is of order 10^{13} GeV. The inverse exponential potential therefore emerges as a compelling candidate for early-Universe inflation, combining theoretical simplicity with robust observational viability.

Keywords: inflation, early universe, cosmic microwave background

Contents

1	Introduction	1
2	Inverse exponential inflationary potential	2
3	Consistency with Observations	3
3.1	Energy scale of inflation	6
4	Post-inflationary dynamics and reheating	6
4.1	Reheating temperature	8
5	Conclusions	10
A	Inflationary and late-time tracker potentials	11

1 Introduction

Inflation [1–4] generically predicts a nearly scale-invariant spectrum of primordial perturbations, commonly characterized by the scalar spectral index n_s . Measurements of the cosmic microwave background (CMB) by Planck 2018 (P) constrained this quantity to be $n_s = 0.9651 \pm 0.0044$ [5, 6]. More recent observations have revised this picture. The sixth data release (DR6) of the Atacama Cosmology Telescope (ACT) [7, 8] reports $n_s = 0.9666 \pm 0.0077$. When Planck and ACT data are combined with measurements from the Dark Energy Spectroscopic Instrument (DESI) DR1 (DESI1) [9, 10] and DR2 (DESI2) [11], the preferred value shifts significantly toward larger values, yielding $n_s = 0.9743 \pm 0.0034$ [7]. In particular, P–ACT combined with DESI-DR1 (P–ACT–DESI1) gives $n_s = 0.9743 \pm 0.0034$, while inclusion of DESI-DR2 (P–ACT–DESI2) gives $n_s = 0.9752 \pm 0.0030$ [7], differing from the original Planck result by nearly 2σ . Independent measurements from the South Pole Telescope with its third-generation camera (SPT-3G) yield $n_s = 0.951 \pm 0.011$ [12], consistent within uncertainties of Planck measurements. Combining SPT-3G with Planck and ACT-DR6 (SPA) gives $n_s = 0.9684 \pm 0.0030$ [12], and adding DESI-DR2 data (SPA-DESI2) leads to $n_s = 0.9728 \pm 0.0027$ [12]. Incorporating BICEP/Keck B-mode data [13], the SPA-BK combination gives $n_s = 0.9682 \pm 0.0032$ [14], while the SPA-BK-DESI2 dataset yields $n_s = 0.9728 \pm 0.0029$ [14]. The same combination constrains the tensor-to-scalar ratio to $r < 0.035$ [14].

These updated constraints, particularly those including DESI data, place increasing pressure on standard single-field inflationary scenarios. The R^2 Starobinsky model [2, 15], previously favoured by Planck 2018 [5], lies near the boundary of the 2σ allowed region of n_s from P–ACT–BK–DESI1 [8] and SPA–BK–DESI2 [14] for $N = 60$ e-folds, and becomes disfavoured at more than 2σ for smaller N . Monomial inflationary models ϕ^n [3, 4] can accommodate SPA–BK–DESI2 data only at 2σ level for sufficiently small

powers, roughly $n < 1/3$. Consequently, many recent works have explored modifications or extensions of standard scenarios [14, 16–38] to reconcile theoretical predictions with current observational data. However, a simple single-field model consistent with the recent SPA-BK-DESI2 constraint on n_s is still lacking. Here, by *simple* we mean inflation driven by a minimally coupled canonical scalar field with a potential that remains monotonic at least during inflation. Motivated by this, we propose an inverse exponential (IExp) potential of the form $e^{-\alpha/\phi}$ with constant parameter α . Our construction is guided by a comparison between inflationary potentials and tracker potentials [39–42], which are relevant for late time scalar field dynamics. In particular, we analyse the curvature parameter Γ , related to the second slow-roll parameter η_V , together with the slope parameter λ , related to ϵ_V through $\epsilon_V = \lambda^2/2$. Observationally viable inflation requires moderate to large negative Γ , whereas tracker behaviour arises when $\Gamma > 1$. Thus, inflationary and tracker dynamics appear as opposite regimes for large $|\Gamma|$. If one can identify potentials with small $|\lambda|$ and large Γ , then a reflection of Γ naturally yields potentials suitable for inflation.

For the IExp potential, one obtains $\lambda = -\alpha/\phi^2$ and $\Gamma = 1 - 2\phi/\alpha$. For $\alpha < 0$ and $\phi > 0$, the potential exhibits tracker behaviour [39, 42] when ϕ is large, since λ becomes small while Γ becomes sufficiently large and positive. By instead considering $\alpha > 0$, this behaviour is effectively reflected, mapping large positive Γ values to large negative ones while keeping $|\lambda|$ small. This provides a suitable inflationary potential consistent with current observational requirements. In this sense, concave inflationary potentials may act as counterparts of late time tracker potentials, and we therefore may refer to such concave inflationary potentials as anti-tracker potentials, since they correspond, to some extent, to a reflection of the values of the Γ parameter.

2 Inverse exponential inflationary potential

Motivated by the need for inflationary potentials that simultaneously produce a small tensor-to-scalar ratio and a scalar spectral index consistent with current observations, we consider an IExp potential of the form

$$V(\phi) = V_0 e^{-\alpha M_{\text{Pl}}/\phi}, \quad (2.1)$$

where V_0 sets the energy scale of inflation and α is a dimensionless parameter. The potential is assumed to be valid throughout the inflationary regime with $\phi/M_{\text{Pl}} > 0$.

For this potential, the slope and curvature parameters,

$$\lambda = -\frac{M_{\text{Pl}} V'}{V}, \quad \Gamma = \frac{V'' V}{V'^2}, \quad (2.2)$$

take the simple forms

$$\lambda = \frac{\alpha}{\phi^2}, \quad \Gamma = 1 - \frac{2\phi}{\alpha}. \quad (2.3)$$

For $\alpha > 0$ and sufficiently large ϕ , the slope parameter becomes small while the curvature parameter takes large negative values, corresponding to a strongly concave

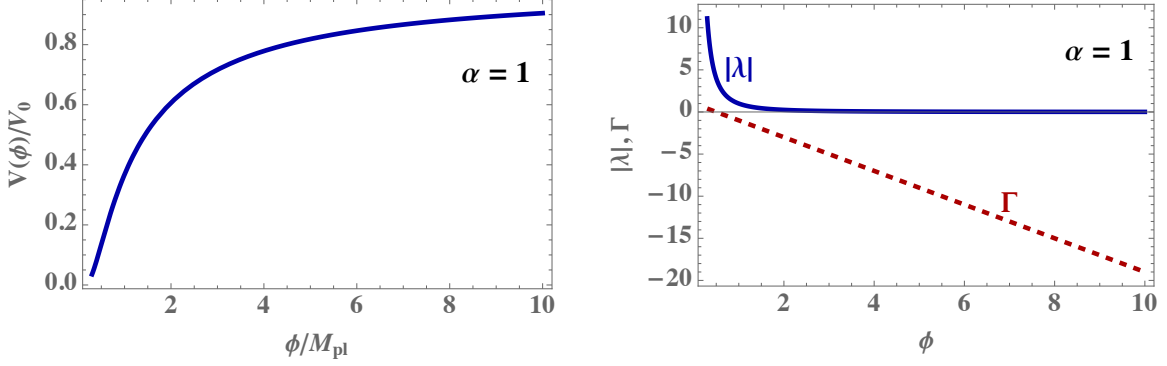


Figure 1: Nature of the potential (2.1) and its slope (λ) and curvature (Γ) for $\phi/M_{\text{Pl}} > 0$ with $\alpha = 1$.

potential suitable for slow-roll inflation. A more general discussion on this is provided in Appendix A.

The behaviour of the potential, together with the corresponding slope and curvature parameters, is shown in Fig. 1. One observes that $|\lambda|$ decreases rapidly with increasing field value, while Γ becomes increasingly negative, satisfying the qualitative conditions required for viable inflation.

Since the potential is singular at $\phi = 0$, modifications are required to describe post-inflationary dynamics. Such modifications and their consequences for reheating will be discussed later in Sec. 4.

3 Consistency with Observations

The potential slow-roll parameters for the potential (2.1) take the explicit form

$$\epsilon_V(\phi) = \frac{\alpha^2 M_{\text{Pl}}^4}{2\phi^4}, \quad (3.1)$$

$$\eta_V(\phi) = \frac{\alpha M_{\text{Pl}}^3}{\phi^3} \left(\frac{\alpha M_{\text{Pl}}}{\phi} - 2 \right), \quad (3.2)$$

$$\xi_V^2(\phi) = \frac{\alpha^2 M_{\text{Pl}}^4}{\phi^8} (\alpha^2 M_{\text{Pl}}^2 - 6\alpha M_{\text{Pl}}\phi + 6\phi^2). \quad (3.3)$$

Inflation ends when the slow-roll condition $\epsilon_V = 1$ is violated, which fixes the field value at the end of inflation as

$$\phi_{\text{end}} = \left(\frac{\sqrt{\alpha}}{2^{1/4}} \right) M_{\text{Pl}}. \quad (3.4)$$

The number of e -folds between a field value ϕ_* (corresponding to horizon exit of the pivot scale) and ϕ_{end} is given by

$$N_* = \int_{t_*}^{t_{\text{end}}} H dt \simeq \frac{1}{M_{\text{Pl}}^2} \int_{\phi_{\text{end}}}^{\phi_*} \frac{V}{V_{,\phi}} d\phi = \frac{1}{3\alpha M_{\text{Pl}}^3} (\phi_*^3 - \phi_{\text{end}}^3), \quad (3.5)$$

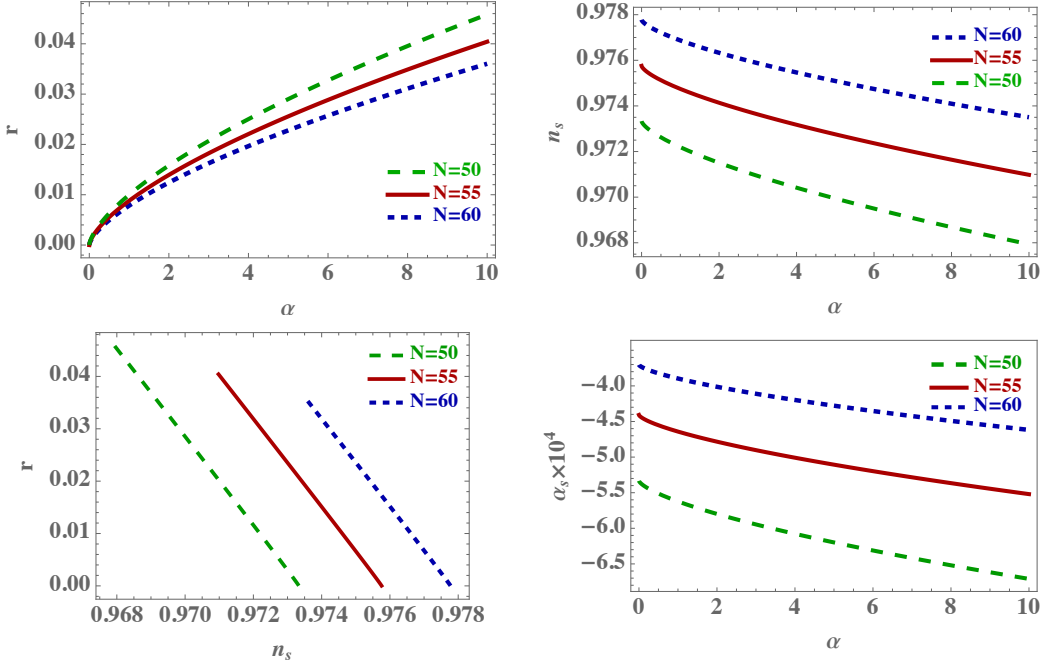


Figure 2: Inflation parameters for the potential (2.1) for $\phi/M_{\text{Pl}} > 0$. For all the plots $0.05 \leq \alpha \leq 10$.

which determines ϕ_* for a given N_*

$$\phi_* = M_{\text{Pl}} \left[3\alpha N_* + \left(\frac{\alpha^2}{2} \right)^{3/4} \right]^{1/3}, \quad (3.6)$$

For $N_* \gg \alpha$, this simplifies to

$$\phi_* \simeq (3\alpha N_*)^{1/3} M_{\text{Pl}}. \quad (3.7)$$

Evaluated at ϕ_* , the inflationary observables at leading order in slow roll are

$$r = 16\epsilon_V(\phi_*) = \frac{8\alpha^2 M_{\text{Pl}}^4}{\phi_*^4}, \quad (3.8)$$

$$n_s = 1 - 6\epsilon_V(\phi_*) + 2\eta_V(\phi_*) = 1 - \frac{\alpha^2 M_{\text{Pl}}^4}{\phi_*^4} - \frac{4\alpha M_{\text{Pl}}^3}{\phi_*^3}, \quad (3.9)$$

$$\alpha_s \equiv \frac{dn_s}{d \ln k} = 16\epsilon_V \eta_V - 24\epsilon_V^2 - 2\xi_V^2 = -\frac{4\alpha^2 M_{\text{Pl}}^6 (\alpha M_{\text{Pl}} + 3\phi_*)}{\phi_*^7}. \quad (3.10)$$

Figure 2 shows the dependence of the inflationary observables, the tensor-to-scalar ratio r , the scalar spectral index n_s , and the running of the scalar spectral index α_s , on the model parameter α . These observables are evaluated at horizon exit for $N = 50$ –60 e-folds. We find that over a wide range of α , the model predicts a sufficiently small tensor-to-scalar ratio r , while the scalar spectral index remains

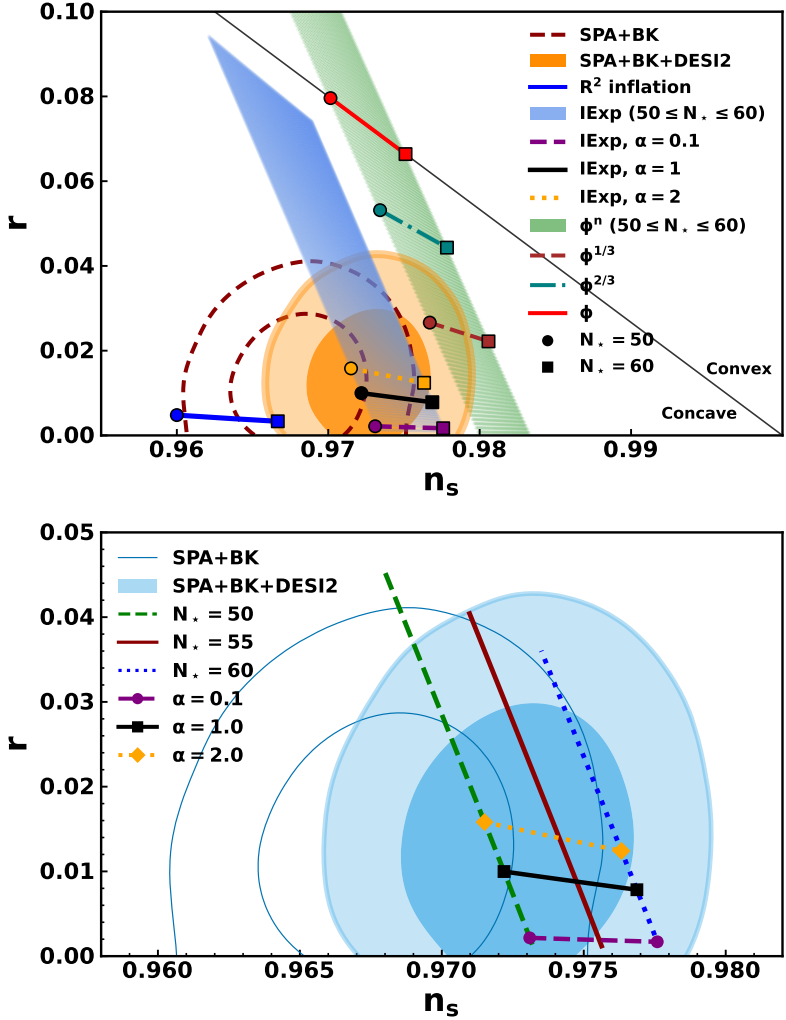


Figure 3: Comparison of the theoretical prediction of tensor-to-scalar ratio r and the scalar spectral index n_s with the observational results for $N_* = 50-60$. In the upper figure, along with our model we have also shown the predictions from the R^2 Starobinsky inflationary model and monomial inflationary model. The bottom figure shows a magnified view of the upper panel, highlighting the predictions of our model for $N_* = 50-60$. For the contours we use publicly available MCMC chains [14].

clustered around $n_s \simeq 0.97$, consistent with current observational constraints. The lower-right panel further shows that the running of the scalar spectral index is nearly negligible across the considered parameter range.

In Fig. 3, we compare the inflationary predictions of the potential (2.1) in the (n_s, r) plane with the observational constraints. For completeness, we also display the predictions of the R^2 inflation [2, 15, 43] and representative monomial inflationary potentials [4]. The shaded contours correspond to the combined SPA+BK+DESI2 data set, while the line contours represent the SPA+BK constraints. For the contours

in the Fig. 3 we use publicly available MCMC chains¹ [14] and visualised using the `GetDist` package [44].

We find that the predictions of our model lie well within the 1σ confidence region of the SPA+BK+DESI2 contours for a broad range of the parameter α , demonstrating excellent agreement with the observational data. In contrast, the R^2 inflation model and the monomial potentials considered here lie partially or entirely outside the 2σ region and are therefore comparatively disfavoured by the current data.

3.1 Energy scale of inflation

In the slow-roll approximation, the amplitude of the scalar power spectrum at horizon crossing ($k = k_* = a_* H_*$) is given by

$$A_s(k_*) = \frac{1}{24\pi^2} \frac{V_*}{\epsilon_V(\phi_*) M_{\text{Pl}}^4}, \quad (3.11)$$

where $V_* = V(\phi_*)$. The Planck collaboration constrains the scalar amplitude at the pivot scale $k_* = 0.05 \text{ Mpc}^{-1}$ to be [5]

$$A_s(k_*) = 2.10 \times 10^{-9}. \quad (3.12)$$

Using Eqs. (3.11) and (3.12), the inflationary energy scale can be written as

$$V_*^{1/4} = (24\pi^2 A_s \epsilon_V(\phi_*))^{1/4} M_{\text{Pl}} = \left(\frac{3}{2}\pi^2 r A_s\right)^{1/4} M_{\text{Pl}} = 3.233 \times 10^{16} r^{1/4} \text{ GeV}. \quad (3.13)$$

which gives us $V_*^{1/4} = 1.02 \times 10^{16} \text{ GeV}$ for $r = 0.01$.

4 Post-inflationary dynamics and reheating

To ensure a graceful exit from inflation and a consistent reheating phase, we extend the inflationary potential (2.1) by introducing an additional exponential (Exp) term that becomes relevant after the end of slow-roll inflation. The resulting potential is taken to be

$$V(\phi) = \text{IExp} + \text{Exp} = V_0 \left(e^{-\alpha M_{\text{Pl}}/\phi} + e^{-\beta\phi/M_{\text{Pl}}} \right), \quad (4.1)$$

where $\alpha, \beta > 0$. During inflation, the IExp term dominates for sufficiently small field values, thereby reproducing the inflationary dynamics discussed in the previous sections. The Exp term $e^{-\beta\phi/M_{\text{Pl}}}$ becomes important only at later stages and facilitates the transition to reheating. The nature of the potential (4.1) is illustrated in Fig. 4 for $\alpha = 1$ and $\beta = 15$. After the end of inflation at ϕ_{end} , the potential develops a minimum at ϕ_{eq} . The green dot denotes the field value ϕ_{eq} at which the IExp and Exp contributions to the potential (4.1) become equal, while the blue dot marks the field value ϕ_{end} .

¹https://github.com/Lbalkenhol/r_ns_2025

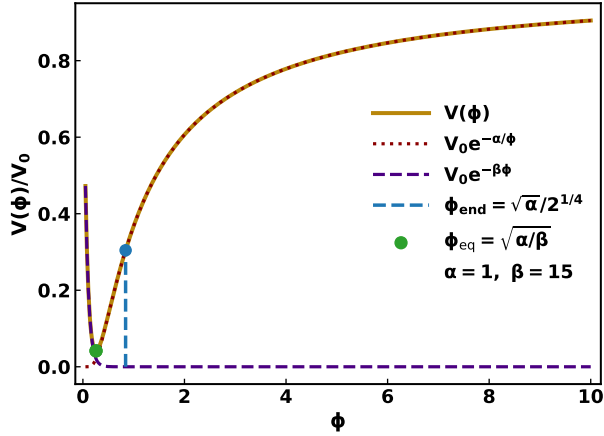


Figure 4: Nature of the full inflationary potential (4.1) for $\alpha = 1$ and $\beta = 15$.

ϕ_{eq} is given by

$$\phi_{\text{eq}} = \sqrt{\frac{\alpha}{\beta}} M_{\text{Pl}}. \quad (4.2)$$

For a viable reheating scenario, the exponential term must become relevant only after the end of inflation. This requirement translates into the condition

$$\phi_{\text{eq}} < \phi_{\text{end}} \implies \beta > \sqrt{2}. \quad (4.3)$$

This bound guarantees that the exponential term $e^{-\beta\phi/M_{\text{Pl}}}$ remains subdominant throughout the inflationary phase. In practice, to ensure that this term is entirely negligible during inflation, one requires

$$e^{-\beta\phi_{\text{end}}/M_{\text{Pl}}} \ll e^{-\alpha M_{\text{Pl}}/\phi_{\text{end}}}, \quad (4.4)$$

which implies $\beta \gg \sqrt{2}$. This behaviour is illustrated in Fig. 5. To estimate the minimum viable value of β for a given α , we solve the full Klein–Gordon equation

$$\ddot{\phi} + 3H\dot{\phi} + V'(\phi) = 0, \quad (4.5)$$

starting from the end of inflation. Since the detailed physics of the reheating era is unknown, we assume, for simplicity, that the scalar field is the sole component of the Universe during this phase.

As the full inflationary potential (4.1) develops a minimum after the end of inflation (see Fig. 4), the scalar field undergoes oscillations about this minimum, a necessary ingredient for successful reheating. This behaviour is shown in the left panel of Fig. 5, where we plot the evolution of the scalar field equation of state w_ϕ as a function of the number of e-folds measured from the end of inflation. Only a portion of the evolution is displayed for clarity. The red dashed line represents the time-averaged equation of state.

In the right panel of Fig. 5, we show the dependence of the time averaged equation of state $\langle w_\phi \rangle$ on the parameter β for $\alpha = 1$. We find that for $\beta \lesssim 20$, $\langle w_\phi \rangle$ remains

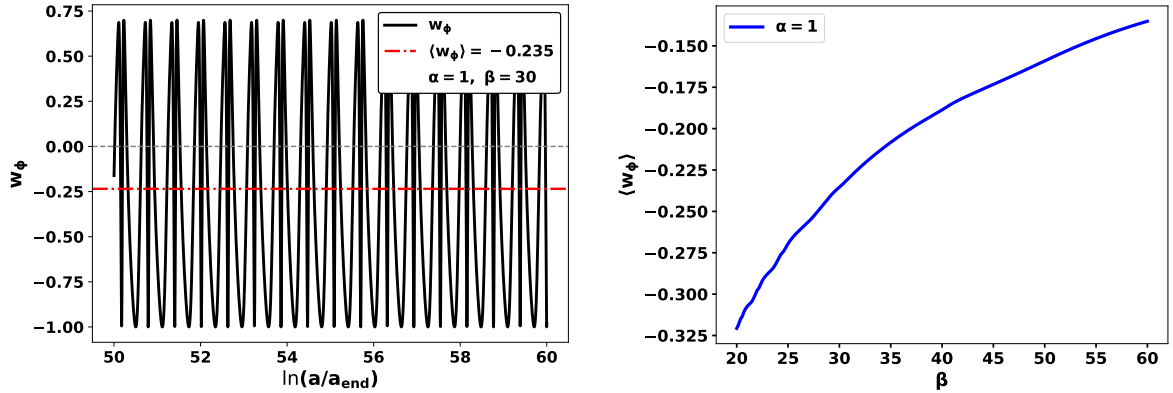


Figure 5: Post-inflationary evolution of the scalar field for the potential (4.1) for $\alpha = 1$ and $\beta = 30$.

close to or below $-1/3$, indicating a prolonged accelerated phase after inflation. This implies that a sufficiently large value of β is required to ensure a graceful exit from inflation, in agreement with the analytical arguments presented above. For a fixed value of α , increasing β leads to a larger average equation of state, $\langle w_\phi \rangle$.

4.1 Reheating temperature

After the end of inflation, the inflaton field rolls down the potential and its energy density is transferred to relativistic particles, initiating the reheating phase. The reheating temperature, T_{rh} , is defined as the temperature of the thermal bath at the completion of reheating, when the Universe enters the radiation-dominated era. Assuming instantaneous thermalisation of the inflaton energy density into radiation, the reheating temperature can be written as [45]

$$T_{\text{rh}} = \left(\frac{30}{\pi^2 g_{\text{rh}}} \right)^{1/4} \rho_{\text{rh}}^{1/4}, \quad (4.6)$$

where g_{rh} denotes the effective number of relativistic degrees of freedom at the end of reheating, and ρ_{rh} is the energy density at that time.

The energy density at the end of reheating can be related to the energy density at the end of inflation by assuming that reheating proceeds with a constant effective equation of state parameter w_{rh} . Under this assumption, the energy density evolves as

$$\frac{\rho_{\text{end}}}{\rho_{\text{rh}}} = \left(\frac{a_{\text{end}}}{a_{\text{rh}}} \right)^{-3(1+w_{\text{rh}})}, \quad (4.7)$$

where a_{end} and a_{rh} are the scale factors at the end of inflation and at the end of reheating, respectively.

At the end of inflation, when the equation of state approaches $w = -1/3$, the total energy density is related to the potential energy as $\rho_{\text{end}} = \frac{3}{2}V_{\text{end}}$. The number of

e-folds during reheating, N_{rh} , defined as the interval between the end of inflation and the onset of the radiation-dominated epoch ($w = 1/3$), is then given by

$$\begin{aligned} N_{\text{rh}} &= \ln\left(\frac{a_{\text{rh}}}{a_{\text{end}}}\right) = \frac{1}{3(1+w_{\text{rh}})} \ln\left(\frac{\rho_{\text{end}}}{\rho_{\text{rh}}}\right) \\ &= \frac{1}{3(1+w_{\text{rh}})} \ln\left(\frac{3}{2} \frac{V_{\text{end}}}{\rho_{\text{rh}}}\right). \end{aligned} \quad (4.8)$$

For $g_{\text{rh}} \simeq 100$,

$$\ln\left[\left(\frac{43}{11g_{\text{rh}}}\right)^{1/3} \frac{a_0 T_0}{k_*}\right] \approx 61.6, \quad (4.9)$$

where a_0 and $T_0 = 2.73$ K denote the present day scale factor and CMB temperature, $k_* = 0.05 \text{ Mpc}^{-1}$ is the pivot scale. Using the above result the reheating e-fold number can be expressed in terms of inflationary observables as [45]

$$N_{\text{rh}} = \frac{4}{1-3w_{\text{rh}}} \left[61.6 - \ln\left(\frac{V_{\text{end}}^{1/4}}{H_*}\right) - N_* \right], \quad (4.10)$$

valid for $w_{\text{rh}} \neq 1/3$. Here, $H_* = \pi\sqrt{rA_s(k_*)/2} M_{\text{Pl}}$ is the Hubble parameter at the horizon crossing of the pivot scale, and N_* is given by Eq. (3.5).

Using Eq. (4.8) and (4.6) the reheating temperature can be represented as

$$T_{\text{rh}} = \left(\frac{45V_{\text{end}}}{\pi^2 g_{\text{rh}}}\right)^{1/4} \exp\left[-\frac{3}{4}(1+w_{\text{rh}}) N_{\text{rh}}\right]. \quad (4.11)$$

which, using Eq. (4.10) along with Eq. (4.9), becomes [45]

$$T_{\text{rh}} = \left[\left(\frac{43}{11g_{\text{rh}}}\right)^{1/3} \frac{a_0 T_0}{k_*} H_* e^{-N} \left(\frac{45V_{\text{end}}}{\pi^2 g_{\text{rh}}}\right)^{-\frac{1}{3(1+w_{\text{rh}})}}\right]^{\frac{3(1+w_{\text{rh}})}{3w_{\text{rh}}-1}}, \quad (4.12)$$

again for $w_{\text{rh}} \neq 1/3$.

Figures 6 display the reheating e-folding number and reheating temperature obtained for different reheating equations of state, $w_\phi = -0.33, -0.1, 0$, and 0.2 . As α increases, the allowed region shifts toward smaller values of the scalar spectral index n_s . Nevertheless, for all considered cases, the predicted reheating temperatures remain consistent with the observationally allowed 1σ range of n_s .

The maximum reheating temperature predicted by the model typically lies in the range $T_{\text{rh}} \sim 10^{12}\text{--}10^{13}$ GeV. On the lower side, the minimum reheating temperature compatible with the 1σ constraint on n_s depends on α , reaching values as small as $\sim 10^{-9}$ GeV for $\alpha = 1$ and 5 , while increasing to values of order a few GeV for larger α within the same 1σ bound on n_s . Lower reheating temperatures are generally allowed for smaller values of α and larger values of w_ϕ , whereas, overall, larger reheating temperatures are more strongly favoured within the observationally preferred parameter space.

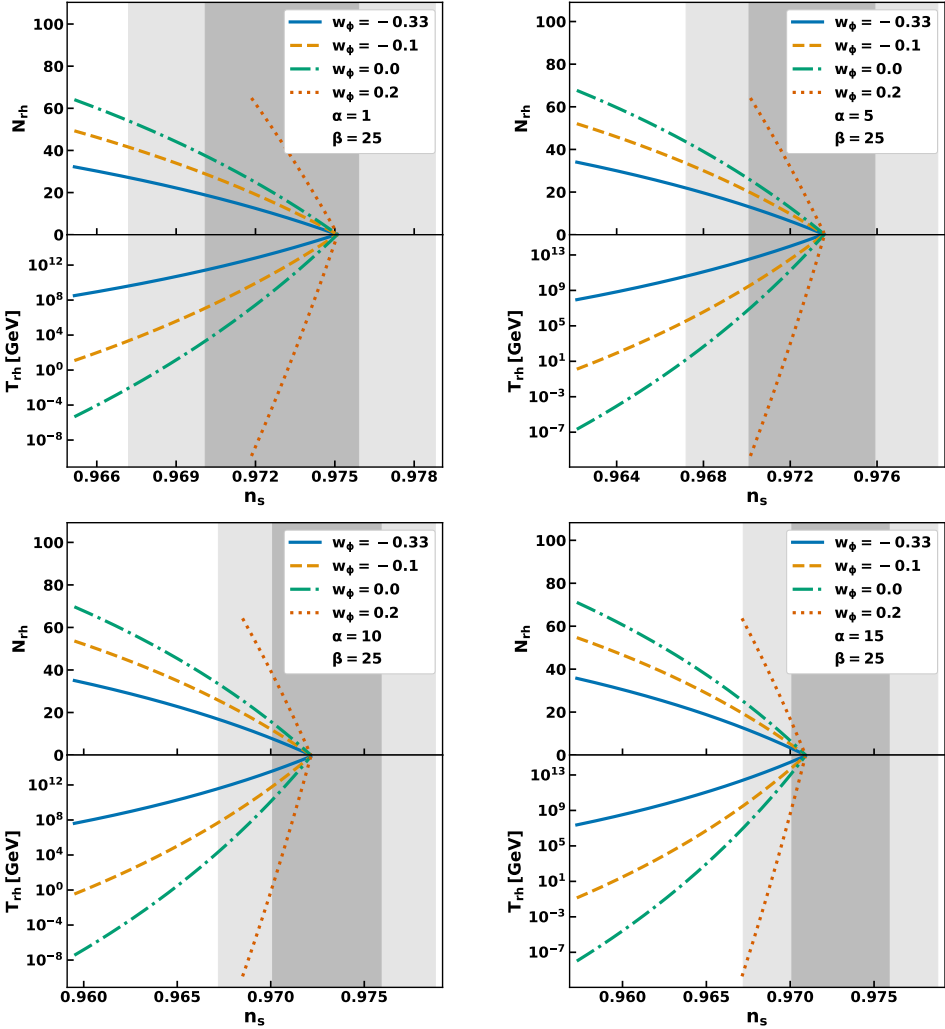


Figure 6: Reheating e-folding number and reheating temperature predicted by the potential (4.1) for different values of α , with $\beta = 25$. Each panel corresponds to a specific choice of α , showing how the reheating dynamics vary with the inflationary parameters of the model.

5 Conclusions

We have investigated an inflationary scenario based on the IExp potential (2.1), motivated by its connection to tracker dynamics familiar from late-time cosmology. Analytic expressions for the slow-roll parameters and inflationary observables were derived, showing that for a wide range of the model parameter α , the predicted scalar spectral index n_s and tensor-to-scalar ratio r lie comfortably within current observational constraints from the combined SPA+BK+DESI data set. In particular, the model satisfies the upper bound $r < 0.035$ from SPA+BK+DESI2, while simultaneously predicting n_s values fully consistent with the same data set (see Figs. 2 and 3). The running of the scalar spectral index is found to be nearly negligible across the parameter space

(bottom-right panel of Fig. 2), in agreement with observational expectations.

These results demonstrate that the potential (2.1) provides a simple and viable single-field inflationary scenario that naturally satisfies current observational bounds. Its minimalistic form, comprising a canonical scalar field with a single exponential term, addresses the observationally imposed challenge of identifying a simple, empirically favoured single field model of inflation. The IExp potential therefore emerges as a compelling candidate for early-Universe inflation, uniting theoretical simplicity with robust agreement with data.

To ensure a graceful exit from inflation and a consistent post-inflationary evolution, we extended the inflationary potential by adding an exponential term (Eq. (4.1)) that becomes relevant only after the end of slow roll. This extension generates a minimum in the potential, allowing the scalar field to oscillate and enabling reheating (Fig. 5). We analysed the resulting post-inflationary dynamics and showed that successful reheating requires sufficiently large values of the parameter β , ensuring that the additional exponential contribution remains negligible during inflation but dominates afterwards.

Using standard reheating parametrisation, we also computed the reheating e-fold number and reheating temperature for various reheating equations of state (Fig. 6). The predicted reheating temperatures remain compatible with observational bounds derived from the allowed range of n_s , with typical maximum values around 10^{12} – 10^{13} GeV, while lower temperatures remain viable depending on model parameters.

A Inflationary and late-time tracker potentials

Under the slow-roll approximation, inflation driven by a canonical scalar field is characterized by the potential slow-roll parameters

$$\epsilon_V = \frac{M_{\text{Pl}}^2}{2} \left(\frac{V'}{V} \right)^2, \quad \eta_V = M_{\text{Pl}}^2 \frac{V''}{V}. \quad (\text{A.1})$$

The inflationary observables are then

$$n_s = 1 - 6\epsilon_V + 2\eta_V, \quad r = 16\epsilon_V. \quad (\text{A.2})$$

Although observations require both slow-roll parameters to be small, this formulation does not directly clarify the required shape of the potential.

It is therefore convenient to introduce the slope and curvature parameters

$$\lambda = -\frac{M_{\text{Pl}} V'}{V}, \quad \Gamma = \frac{V'' V}{V'^2}, \quad (\text{A.3})$$

for which

$$\epsilon_V = \frac{\lambda^2}{2}, \quad \eta_V = \lambda^2 \Gamma, \quad (\text{A.4})$$

and

$$n_s = 1 - \lambda^2(3 - 2\Gamma), \quad r = 8\lambda^2. \quad (\text{A.5})$$

Table 1: Allowed values of the potential flow parameters λ and Γ , together with the corresponding slow-roll parameters ϵ_V and η_V , for representative values of r assuming $0.95 < n_s < 0.98$.

$0.95 < n_s < 0.98$	$r = 0.034$	$\epsilon_V \simeq 0.021$ $-0.018 \lesssim \eta_V \lesssim -0.0038$	$\lambda \simeq 0.065$ $-4.4 \lesssim \Gamma \lesssim -0.9$
	$r = 0.01$	$\epsilon_V \simeq 0.00063$ $-0.023 \lesssim \eta_V \lesssim -0.0081$	$\lambda \simeq 0.035$ $-18.5 \lesssim \Gamma \lesssim -6.5$
	$r = 0.005$	$\epsilon_V \simeq 0.00031$ $-0.024 \lesssim \eta_V \lesssim -0.0091$	$\lambda \simeq 0.025$ $-38.5 \lesssim \Gamma \lesssim -14.5$

Using observational constraints on n_s and representative values of r , one can map the allowed regions in (λ, Γ) space. The resulting ranges are summarized in Table 1. These results indicate that viable single-field inflation requires a small slope parameter together with moderate to large negative Γ , implying that the inflationary potential must be strongly concave.

In late-time scalar-field cosmology, tracker solutions arise when $\Gamma > 1$. Inflation instead requires $\Gamma < 0$, suggesting that inflationary potentials can be viewed as approximate reflections of tracker potentials in Γ . We therefore refer to such concave inflationary potentials as anti-tracker potentials.

This correspondence is illustrated using familiar examples. Monomial potentials ϕ^n behave as anti-tracker counterparts of inverse power-law tracker potentials ϕ^{-n} , while a generalized Starobinsky potential $(1 + \xi e^{-\sqrt{2/3}\phi})^2$ exhibits mirrored behaviour in Γ for $\xi = \pm 1$, as shown in Fig. 7. The mirrored behaviour appears in the region where $|\lambda|$ is small, corresponding to the field range relevant for inflation.

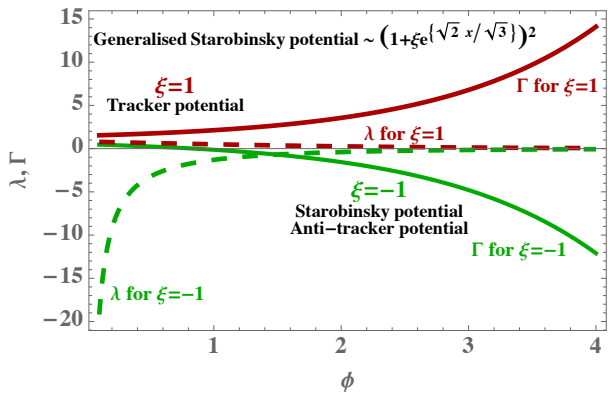


Figure 7: Evolution of the slope λ (dashed lines) and curvature parameter Γ (solid lines) as functions of the scalar field for the generalized Starobinsky potential. Green curves correspond to $\xi = -1$ (Starobinsky inflation) and red curves to $\xi = 1$ (tracker counterpart).

References

- [1] A.H. Guth, *The Inflationary Universe: A Possible Solution to the Horizon and Flatness Problems*, *Phys. Rev. D* **23** (1981) 347.
- [2] A.A. Starobinsky, *A New Type of Isotropic Cosmological Models Without Singularity*, *Phys. Lett. B* **91** (1980) 99.
- [3] A.D. Linde, *A New Inflationary Universe Scenario: A Possible Solution of the Horizon, Flatness, Homogeneity, Isotropy and Primordial Monopole Problems*, *Phys. Lett. B* **108** (1982) 389.
- [4] A.D. Linde, *Chaotic Inflation*, *Phys. Lett. B* **129** (1983) 177.
- [5] PLANCK collaboration, *Planck 2018 results. X. Constraints on inflation*, *Astron. Astrophys.* **641** (2020) A10 [[1807.06211](#)].
- [6] PLANCK collaboration, *Planck 2018 results. VI. Cosmological parameters*, *Astron. Astrophys.* **641** (2020) A6 [[1807.06209](#)].
- [7] ATACAMA COSMOLOGY TELESCOPE collaboration, *The Atacama Cosmology Telescope: DR6 power spectra, likelihoods and Λ CDM parameters*, *JCAP* **11** (2025) 062 [[2503.14452](#)].
- [8] ATACAMA COSMOLOGY TELESCOPE collaboration, *The Atacama Cosmology Telescope: DR6 constraints on extended cosmological models*, *JCAP* **11** (2025) 063 [[2503.14454](#)].
- [9] DESI collaboration, *DESI 2024 III: baryon acoustic oscillations from galaxies and quasars*, *JCAP* **04** (2025) 012 [[2404.03000](#)].
- [10] DESI collaboration, *DESI 2024 VI: cosmological constraints from the measurements of baryon acoustic oscillations*, *JCAP* **02** (2025) 021 [[2404.03002](#)].
- [11] DESI collaboration, *DESI DR2 Results II: Measurements of Baryon Acoustic Oscillations and Cosmological Constraints*, [2503.14738](#).
- [12] SPT-3G collaboration, *SPT-3G D1: CMB temperature and polarization power spectra and cosmology from 2019 and 2020 observations of the SPT-3G Main field*, [2506.20707](#).
- [13] BICEP, KECK collaboration, *Improved Constraints on Primordial Gravitational Waves using Planck, WMAP, and BICEP/Keck Observations through the 2018 Observing Season*, *Phys. Rev. Lett.* **127** (2021) 151301 [[2110.00483](#)].
- [14] L. Balkenhol et al., *Inflation at the End of 2025: Constraints on r and n_s Using the Latest CMB and BAO Data*, [2512.10613](#).
- [15] A.A. Starobinsky, *The Perturbation Spectrum Evolving from a Nonsingular Initially De-Sitter Cosmology and the Microwave Background Anisotropy*, *Sov. Astron. Lett.* **9** (1983) 302.
- [16] R. Kallosh, A. Linde and D. Roest, *Atacama Cosmology Telescope, South Pole Telescope, and Chaotic Inflation*, *Phys. Rev. Lett.* **135** (2025) 161001 [[2503.21030](#)].
- [17] S. Aoki, H. Otsuka and R. Yanagita, *Higgs-modular inflation*, *Phys. Rev. D* **112** (2025) 043505 [[2504.01622](#)].

[18] A. Berera, S. Brahma, Z. Qiu, R. O. Ramos and G.S. Rodrigues, *The early universe is ACT-ing warm*, *JCAP* **11** (2025) 059 [[2504.02655](#)].

[19] C. Dioguardi, A.J. Iovino and A. Racioppi, *Fractional attractors in light of the latest ACT observations*, *Phys. Lett. B* **868** (2025) 139664 [[2504.02809](#)].

[20] A. Salvio, *Independent connection in action during inflation*, *Phys. Rev. D* **112** (2025) L061301 [[2504.10488](#)].

[21] C. Dioguardi and A. Karam, *Palatini linear attractors are back in action*, *Phys. Rev. D* **111** (2025) 123521 [[2504.12937](#)].

[22] M.U. Rehman and Q. Shafi, *Supersymmetric hybrid inflation in light of the Atacama Cosmology Telescope data release 6, Planck 2018, and LB-BK18*, *Phys. Rev. D* **112** (2025) 023529 [[2504.14831](#)].

[23] Q. Gao, Y. Gong, Z. Yi and F. Zhang, *Nonminimal coupling in light of ACT data*, *Phys. Dark Univ.* **50** (2025) 102106 [[2504.15218](#)].

[24] M. He, M. Hong and K. Mukaida, *Increase of ns in regularized pole inflation & Einstein-Cartan gravity*, *JCAP* **09** (2025) 080 [[2504.16069](#)].

[25] I.D. Gialamas, A. Karam, A. Racioppi and M. Raidal, *Has ACT measured radiative corrections to the tree-level Higgs-like inflation?*, *Phys. Rev. D* **112** (2025) 103544 [[2504.06002](#)].

[26] R. Kallosh and A. Linde, *On the present status of inflationary cosmology*, *Gen. Rel. Grav.* **57** (2025) 135 [[2505.13646](#)].

[27] M. Drees and Y. Xu, *Refined predictions for Starobinsky inflation and post-inflationary constraints in light of ACT*, *Phys. Lett. B* **867** (2025) 139612 [[2504.20757](#)].

[28] E.G.M. Ferreira, E. McDonough, L. Balkenhol, R. Kallosh, L. Knox and A. Linde, *The BAO-CMB Tension and Implications for Inflation*, [2507.12459](#).

[29] Y. Aldabergenov and S.V. Ketov, *Single-field D-type inflation in the minimal supergravity in light of Planck-ACT-SPT data*, [2512.08760](#).

[30] V. Keus and S.F. King, *Chaotic Inflation RIDES Again*, [2511.05799](#).

[31] R. Kallosh and A. Linde, *Singular α -attractors*, [2512.02969](#).

[32] W.-Y. Ai, S.F. King, X. Wang and Y.-L. Zhou, *Curvaton-assisted hilltop inflation*, [2512.09079](#).

[33] Q.-Y. Wang, *Inflation in light of ACT/SPT: a new perspective from Weyl gravity*, [2512.10862](#).

[34] N. Kumar, G. Otalora, R. Reyes, B. Espinoza, M. Gonzalez-Espinoza and E.N. Saridakis, *Higgs-like inflation in scalar-torsion $f(T, \phi)$ gravity in light of ACT-SPT-DESI constraints*, [2512.24502](#).

[35] A. Racioppi, *Exponential plateaus and inflation in metric-affine gravity*, [2512.16815](#).

[36] W. Ahmed, W. Ahmad, A. Illahi and M. Junaid, *Warm Hybrid Axion Inflation in α -Attractor Models Constrained by ACT and Future Plan experiments*, [2601.10145](#).

[37] R. Herrera and C. Ríos, *Reconstructing inflation in Einstein-Gauss-Bonnet gravity in light of ACT data*, [2601.18958](#).

- [38] S.D. Odintsov and V.K. Oikonomou, *\mathcal{R}^2 -corrected Tachyon Scalar Field Inflation, the ACT Data, and Phantom Transition*, [2601.21364](#).
- [39] P.J. Steinhardt, L.-M. Wang and I. Zlatev, *Cosmological tracking solutions*, *Phys. Rev. D* **59** (1999) 123504 [[astro-ph/9812313](#)].
- [40] I. Zlatev, L.-M. Wang and P.J. Steinhardt, *Quintessence, cosmic coincidence, and the cosmological constant*, *Phys. Rev. Lett.* **82** (1999) 896 [[astro-ph/9807002](#)].
- [41] M.W. Hossain and A. Maqsood, *Comparison between axionlike and power law potentials in a cosmological background*, *Phys. Rev. D* **109** (2024) 103512 [[2311.17825](#)].
- [42] M.W. Hossain and A. Maqsood, *Cosmological implications of tracker scalar fields: Testing the evidence for dynamical dark energy with recent data*, *Phys. Rev. D* **112** (2025) 083504 [[2502.19274](#)].
- [43] V.F. Mukhanov and G.V. Chibisov, *Quantum Fluctuations and a Nonsingular Universe*, *JETP Lett.* **33** (1981) 532.
- [44] A. Lewis, *GetDist: a Python package for analysing Monte Carlo samples*, [1910.13970](#).
- [45] J.L. Cook, E. Dimastrogiovanni, D.A. Easson and L.M. Krauss, *Reheating predictions in single field inflation*, *JCAP* **04** (2015) 047 [[1502.04673](#)].